Biochemical Analysis of Actin in Crane-fly Gonial Cells: Evidence for Actin in Spermatocytes and Spermatids—but Not Sperm

ARTHUR R. STRAUCH, ELIZABETH J. LUNA, and JAMES R. LAFOUNTAIN, JR.
Division of Cell and Molecular Biology, State University of New York at Buffalo, Buffalo, New York 14260, and The Biological Laboratories, Harvard University, Cambridge, Massachusetts 02138

ABSTRACT A biochemical assay employing DNase-I affinity chromatography, two-dimensional peptide analysis, and SDS polyacrylamide gel electrophoresis was used to isolate, identify, and assess the amount of actin from gonial cells of the crane fly, *Nephrotoma suturalis*. Based on the analysis of cell homogenates under conditions in which all cellular actin is converted to the monomeric DNase-binding form, actin comprises ~1% of the total protein in homogenates of spermatocytes and spermatids. SDS gel analysis of mature sperm reveals no polypeptides with a molecular weight similar to that of actin. Under conditions that preserve native supramolecular states of actin, ~80% of the spermatocyte actin is in a sedimentable form whereas only ~30% of the spermatid actin is sedimentable. These differences could be meaningful with regard to structural changes that occur during spermiogenesis. A comparative analysis of two-dimensional peptide maps of several radioiodinated actins reveals similarities among spermatocyte, spermatid, and human erythrocyte actins. The results suggest the general applicability of this approach to other cell types that contain limited amounts of actin.

Actin has been found in a variety of nonmuscle cells (31) and, on that basis, many investigators have suggested that it may be a ubiquitous structural protein involved in several processes including cell locomotion (7, 39), the maintenance of cell shape (6, 35), and cell cleavage (33). Included in the list of actin-containing cells are crane-fly gonial cells (spermatocytes, spermatids, and sperm of *Nephrotoma suturalis*) which have been reported by Forer and Behnke (11, 12) to contain decorated microfilaments after treatment with glycerol and heavy meromyosin (19, 20). Those results raised the possibility that actin may be involved in the morphogenetic events of spermiogenesis. In addition, Forer and Behnke observed microfilaments in spindles of dividing spermatocytes (11). That finding has been cited frequently as evidence in support of the idea that actin may play a role in the mechanism of chromosome transport (10).

In an attempt to corroborate and extend the findings of Forer and Behnke (11, 12), we have conducted a biochemical analysis of the amount and supramolecular organization of actin in crane-fly gonial cells. Homogenates first were prepared in buffers that either stabilized actin pools in their native state or converted all cell actin to the monomeric DNase-binding form (3) and then were analyzed by a combination of DNase affinity chromatography and SDS polyacrylamide gel electrophoresis (PAGE). This approach takes advantage of the specific interaction between actin and DNase I (27) and is especially applicable to cell types that contain limited amounts of actin. 43,000-dalton polypeptides that were isolated with DNase were characterized further by two-dimensional peptide mapping techniques.

We have confirmed the presence of actin in crane-fly spermatocytes and spermatids and determined that its distribution between monomeric and polymerized states changes during spermiogenesis. Polypeptides with molecular weights similar to that of rabbit muscle actin were not detected in SDS gels of mature sperm. Thus, in contrast to the findings of Forer and Behnke (12), our biochemical assay indicates that actin is not a component of crane-fly sperm.

MATERIALS AND METHODS

Crane flies, *N. suturalis*, were cultivated in the laboratory according to the methods previously described by Forer (9). Cultures were maintained at 25°C on a long-day (17 h light/7 h dark) light cycle, and under these conditions, a complete life cycle (adult → larva → pupa → adult) took ~2 mo. The time

THE JOURNAL OF CELL BIOLOGY · VOLUME 86 JULY 1980 315-325

required for a fourth instar larva bearing spermatocytes to molt into a pupa containing spermatids was ~4 d. Adults emerge from pupae ~7–8 d after the pupal molt.

Cell Preparation

Unless otherwise stated, all procedures were performed on ice or in a 4°C cold room. Preparations of spermatocytes, spermatids, and sperm were obtained applying criteria described in Table I from larvae, pupae, and adult virgin males, respectively by first dissecting the organisms in Belar's Ringer solution (2.4 mM $NaHCO_3$, 150 mM NaCl, 3 mM KCl, 2 mM $CaCl_2$, 22 mM dextrose, pH 7.2) and then removing the intact organ containing gonial cells with watchmakers' forceps. Spermatocytes and spermatids were obtained from testes (Table I), and sperm were obtained from vas deferens. Adult testes, which contain other components in addition to sperm, were included in our analysis. However, because of the smallness and fragility of the testes at this stage, no attempt was made to purify the sperm from these preparations.

Cell preparations were made by rupturing the testes or vas deferens on acid-cleaned coverslips and then separating the cells from the surrounding epithelial and adipose tissue. Isolated cells were collected in 1-ml conical glass test tubes and pelleted by centrifugation for 3–5 min at high speed (~1,500 rpm) in a clinical centrifuge. Cell pellets to be assayed for actin were resuspended in either buffer G or buffer S, described below. Cell preparations intended for direct SDS-PAGE analysis were made by resuspending untreated cell pellets in cold protein sample buffer containing 0.1% Triton X-100. All samples were denatured at 100°C for 5 min. In the case of spermatocytes, the cells were solubilized within 10–15 min. Spermatids and sperm preparations required longer periods (up to 1 h), with solubilization of axonemal components occurring during the 5-min denaturation period at 100°C.

The buffer systems used to assay for DNase-binding protein (monomeric actin) in spermatocyte and spermatid homogenates have been described by Blikstad et al. (3). The experimental protocol is illustrated in Fig. 1. Triton X-100 was included in the preparation of homogenates to aid in the disruption of cells. We have considered the possible influence of detergent-activated proteolysis on our results but doubt that it would be significant in the presence of the protease inhibitor phenylmethyl sulfonylfluoride (PMSF). This conclusion is also supported by our unpublished observations that there are very few lysosomes in these nonphagocytosing cells.

Cells to be assayed for total actin were resuspended in buffer G: 10 mM Tris-HCl, 0.75 M guanidine hydrochloride, 0.5 M sodium acetate, 0.5 mM $CaCl_2$, 0.5 mM ATP, 0.5% Triton X-100, 0.01 mM PMSF, pH 7.6. Mildly chaotropic buffer G denatures polymerized actin and results in its depolymerization into free monomers that retain the DNase-binding property (3). The final protein concentration of these preparations was 0.5–0.8 mg/ml (~60 testes/0.4 ml of buffer G). Spermatocytes were extracted in buffer G for 2.5 h at 0–4°C to allow for cell lysis and depolymerization of supramolecular forms of actin. Spermatid preparations were not completely solubilized after 2.5 h and therefore were centrifuged for 3 h at 150,000 *g* to remove insoluble components. Buffer G-treated spermatocyte homogenates and high-speed supernates of buffer G-treated spermatid homogenates were applied directly to DNase-agarose columns.

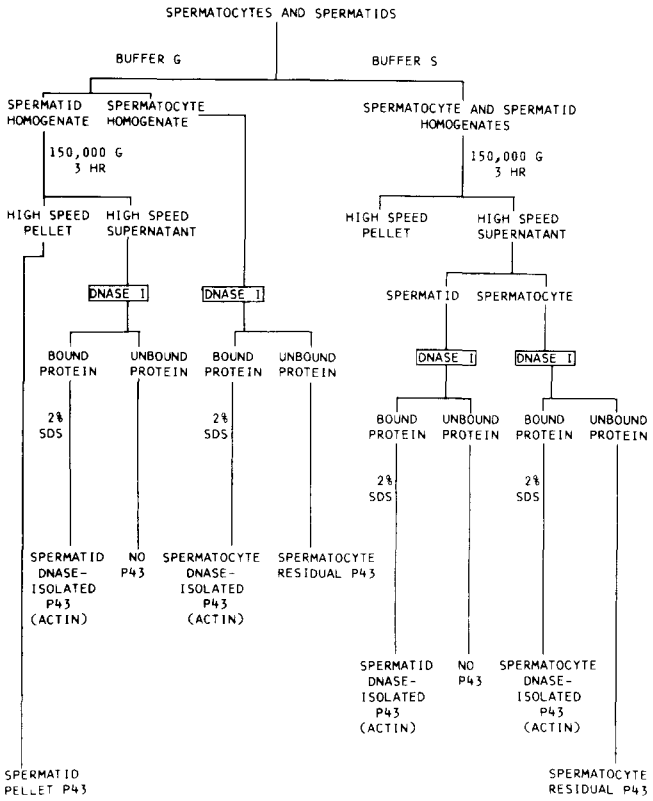

FIGURE 1 Flow chart of experimental protocol for actin assay.

Cells to be assayed for the presence of native monomeric actin were resuspended in buffer S, which stabilizes actin pools in their native state (3). Buffer S: 5 mM Tris-HCl, 0.15 M NaCl, 2 mM $MgCl_2$, 0.2 mM ATP, 0.2 mM dithiothreitol (DTT), 0.5% Triton X-100, 0.01 mM PMSF, pH 7.6. After extraction for 2.5 h at 0–4°C, buffer S-treated spermatocyte and spermatid homogenates, containing 0.5–0.8 mg/ml of protein (~60 testes/0.4 ml of buffer S), were centrifuged for 3 h at 150,000 *g* to pellet supramolecular forms of actin. The efficiency of this centrifugation step was calculated from the relation $S = k/t$, where S is the theoretical sedimentation coefficient (in Svedbergs) of the smallest particle capable of being sedimented during time, t, in a rotor characterized by constant *k*. For a rotor speed of 40,000 rpm and $t_{max} - t_{min} = 1$ cm (Sorvall 865 rotor with a 0.4-ml sample [DuPont Instruments-Sorvall, DuPont Co., Newtown, Conn.]), the *k* factor corresponds to 21. Theoretically, at the end of a 3-h spin, particles larger than 7S should be in the pellet. Using Halsall's equation for the approximation of the molecular weight of a protein from its sedimentation coefficient, $S^0_{20,w} = 0.00242\ M^{0.67}$ (16), a 7S globular protein has a molecular weight of ~150,000 daltons. Under these conditions, all actin oligomers, polymers, and aggregates of four monomer units in size or larger should be in the pellet.

High-speed supernates of buffer S-treated spermatocytes and spermatids were applied to DNase-agarose columns. High-speed pellets were not applied to columns but instead were resuspended to the original volume of homogenate (0.4 ml) with the appropriate buffer used to prepare the homogenate and then denatured with 80 μl of 5× protein sample buffer (see below). By using these volumes to resuspend pellets, gel scans of these fractions could be compared quantitatively to scans of high-speed supernates.

DNase-Agarose Affinity Chromatography

Cyanogen bromide activation of Sepharose 4B (Pharmacia Fine Chemicals, Div. of Pharmacia Inc., Piscataway, N. J.) was performed essentially as described by March et al. (29). The washed, activated agarose slurry was transferred to a DNase-I solution (10 mg DNase I, Worthington type 2006D (Worthington Biochemical Corp., Freehold, N. J.) in 10 ml of 0.1 M sodium bicarbonate, pH 9.0) and coupling was allowed to proceed with gyrotory agitation for 24 h at 0–4°C. The DNase-agarose was then washed initially with 100 vol of 0.1 M sodium bicarbonate, 0.5 M NaCl, pH 9.0, followed by 100 vol of 0.1 M acetic acid, 0.5 M NaCl, pH 3.6, and finally 10 mM Tris-HCl, 0.2 mM $CaCl_2$, 0.5 mM ATP, 0.5 mM DTT, pH 8.0, in which the DNase-agarose was stored at 0–4°C. The amount of DNase coupled per milliliter of agarose was determined by passing a known amount of muscle G-actin through a known volume of DNase-agarose. Assuming a binding stoichiometry of 1:1, ~0.5 mg of DNase was coupled to 1 ml of agarose. For a binding assay on crane-fly homogenates, DNase-agarose was loaded into plastic syringes (0.8 × 2 cm with a 0.4-ml bed volume) and equilibrated with 10 bed volumes of the appropriate buffer. Samples containing 150–350 μg of protein in a 0.4-ml volume were applied to the column and eluted at a flow rate of 0.2 ml/min with either buffer G or buffer S. Because components with a molecular weight below the fractionation range of Sepharose 4B are usually eluted at a volume approximately equal to the total bed volume, fractions of one bed volume each were collected. All unbound protein was collected in the second fraction. After elution of unbound protein, the column was washed with 10 bed volumes of the appropriate buffer containing 1 M NaCl. Both the unbound protein fractions and the salt wash fractions were dialyzed against distilled water for 10 h at 0–4°C after which time 80 μl of 5× protein sample buffer was added and the sample was denatured by heating for 5 min at 100°C. To recover bound material from the column, residual traces of guanidine hydrochloride or NaCl were first removed by washing the column with 10 bed volumes of 5 mM Tris-HCl, 0.2 mM $CaCl_2$, 0.2 mM ATP, 0.2 mM DTT, 0.01 mM PMSF, pH 7.6. Bound protein was then removed by applying one bed volume of 2× protein sample buffer and incubating the agarose-sample buffer slurry for 5 min at 25°C. All denatured protein fractions were analyzed directly with SDS-PAGE.

SDS-PAGE

Analysis of polypeptides was performed on 10% SDS polyacrylamide slab gels with 5% stacking gels according to the procedure of Laemmli (24) using ultrapure reagents from Bio-Rad Laboratories (Richmond, Calif.). Samples were prepared

in a protein sample buffer containing 0.06 M Tris-HCl, 2% SDS, 10% glycerol, 5% β-mercaptoethanol, and 0.001% bromophenol blue, pH 6.8, and denatured for 5 min at 100°C. After the 3–4-h run at 25 mA, gels were fixed and stained in a 50% methanol, 10% acetic acid solution containing 1% Coomassie brilliant blue R (Sigma Chemical Co., St. Louis, Mo.) (21) for 30 min and destained overnight in 10% methanol, 7% acetic acid. Destained gels were scanned directly on a double-beam recording microdensitometer MK IIIC (Joyce, Loebl and Co., Ltd., Gateshead-on-Tyne, England). The amount of protein in a particular band was assessed by comparing the weight of the densitometer scan of that band to the weight of the densitometer scan of the entire gel.

Those approximations were based on the assumption that the dye-to-protein ratio for actin is the same as that for all other polypeptides in a particular gonial cell preparation.

Peptide Mapping

Two-dimensional tryptic mapping of ^{125}I-labeled polypeptides was performed as described by Elder et al. (8), as modified by Kidd et al. (23) and Luna et al. (28). Coomassie blue-stained bands containing ~0.1–3 μg of protein were excised from 10% SDS-polyacrylamide gels. Slices which were mapped included: creatine kinase (Worthington Biochemical Corp.) and ovalbumin (Sigma Chemical Co., grade III), both used without further purification, bovine brain 6S tubulin dimer, prepared by phosphocellulose chromatography (34) of crude microtubule protein obtained by cycles of polymerization and depolymerization (43), purified rabbit skeletal muscle actin (36), human erythrocyte actin extracted at low ionic strength (2), and *Dictyostelium discoideum* actin purified by polymerization from a P6 cytosolic extract fraction according to the method of Hellewell and Taylor (17). Crane-fly p43 polypeptide bands were excised from gels as described in the text.

Electrophoresis of tryptic peptides was carried out for 60 min at 0–2°C and was followed by chromatography in the second dimension for ~3.5 h in the solvent mixture described by Elder et al. (8). Maps were autoradiographed using no screen x-ray film (Eastman Kodak Co., Rochester, N. Y.) with exposures ranging from 4 to 24 h. Only those peptides containing amino acid residues, which can be labeled with ^{125}I in the presence of chloramine-T (tyrosine and, to a lesser extent, histidine and phenylalanine), are visualized by these methods (28).

RESULTS

Micrographs illustrating the different types of cells used in this investigation are included in Fig. 2, and information regarding the composition of these preparations is summarized in Table I. Homogeneous preparations of spermatids and sperm were obtained from pupae and adult males, respectively. Spermatocyte preparations, however, were not homogeneous. Because the meiotic process within the larval testes is not completely synchronous, there were always some spermatids in spermatocyte preparations. Most of the testes that were used for biochemical analysis had a composition similar to that illustrated in Fig. 2 *a*. Some of the testes that met the size criteria (Table I) applied in selecting larval testes contained more spermatids, but even in the most extreme of these cases, not >20% of the total testicular content was occupied by spermatids. Because the volume contribution made by spermatids always was far smaller than that made by spermatocytes, it was unlikely that contamination by spermatids could have had a significant influence on the results obtained with spermatocytes.

Examination of the content of adult testes revealed many unidentified vesicular and rod-shaped components, and significantly fewer sperm than one would expect based on the abundance of spermatids in the pupal testes. The paucity of sperm in adult testes can be explained by the finding that sperm in adult crane flies, like other insects (44), are transported from the testes and held in a vas deferens before ejaculation. Preparations of adult testes were included in our analysis for comparison with results obtained with sperm isolated from vas deferens.

SDS-PAGE analysis of gonial cells revealed that both spermatocyte and spermatid homogenates contained polypeptides that co-migrated with rabbit skeletal muscle actin (Fig. 3 *a* and *b*). On the basis of its apparent molecular weight of 43,000 daltons, we refer to this band, as well as fractionated subsets of this band, as p43. A prominent p43 band was also detected in homogenates of adult testes (Fig. 3 *d*), but it was not detected in homogenates of sperm (Fig. 3 *c*). These results suggest that actin could be present in preparations of spermatocytes, spermatids, and adult testes. However, the absence of a detectable p43 band in our sperm preparations indicated that actin was not a component of sperm.

DNase affinity chromatography was used to isolate actin from spermatocytes and spermatids. Spermatocyte homogenates (Fig. 4 *a*) were prepared in buffer G and then applied to DNase-Sepharose 4B columns. SDS-PAGE analysis of unbound fractions showed a significant reduction in the density of the p43 band (Figs. 4 and 5). Other differences between unfractionated homogenate and the unbound fraction were observed but they are not considered significant because it is believed they are the result of residual traces of guanidine. This reagent probably remained bound to protein subsequent to dialysis and therefore, altered the mobility of SDS-denatured protein. The specific removal of p43 from the homogenate is indicated by the absence of detectable amounts of protein in buffer G fractions containing 1 M NaCl (data not shown) and by the prominent p43 polypeptide found in the fraction removed with 2% SDS (Fig. 4 *c*). Components in the 60,000–70,000-dalton range that are present in the SDS fraction in trace amounts have not been identified. Additional polypeptides in the 15,000–31,000-dalton region were derived from noncovalently bound DNase I and cyanogen bromide breakdown products of DNase I.

Analysis of gel scans of unfractionated spermatocytes (Fig. 5 *a*) has shown that p43 amounts to ~1.6% of the total protein. The residual p43 band remaining after DNase chromatography

TABLE I

Summary of Data on Composition of Cell Preparations

Cell type	Source	Amount	Purity
Spermatocytes (Fig. 2 *a*)	Testis of fourth instar larva (Diameter ≅0.6 mm)	~7 × 10^3 cells/testis (3 μg protein/testis)	>80% spermatocytes with <20% slightly elongated spermatids
Spermatids (Fig. 2 *b*)	Testis of pupa (Diameter ≅0.9 mm)	~2.5 × 10^4 cells/testis (5 μg protein/testis)	100% spermatids
Sperm (Fig. 2 *d*)	Vas deferens of adult	— (2 μg protein/vas deferens)	100% sperm
Sperm (Fig. 2 *c*)	Adult testis (Diameter ≅0.5 mm)	— (0.6 μg protein/testis)	Mainly residual components 10% sperm

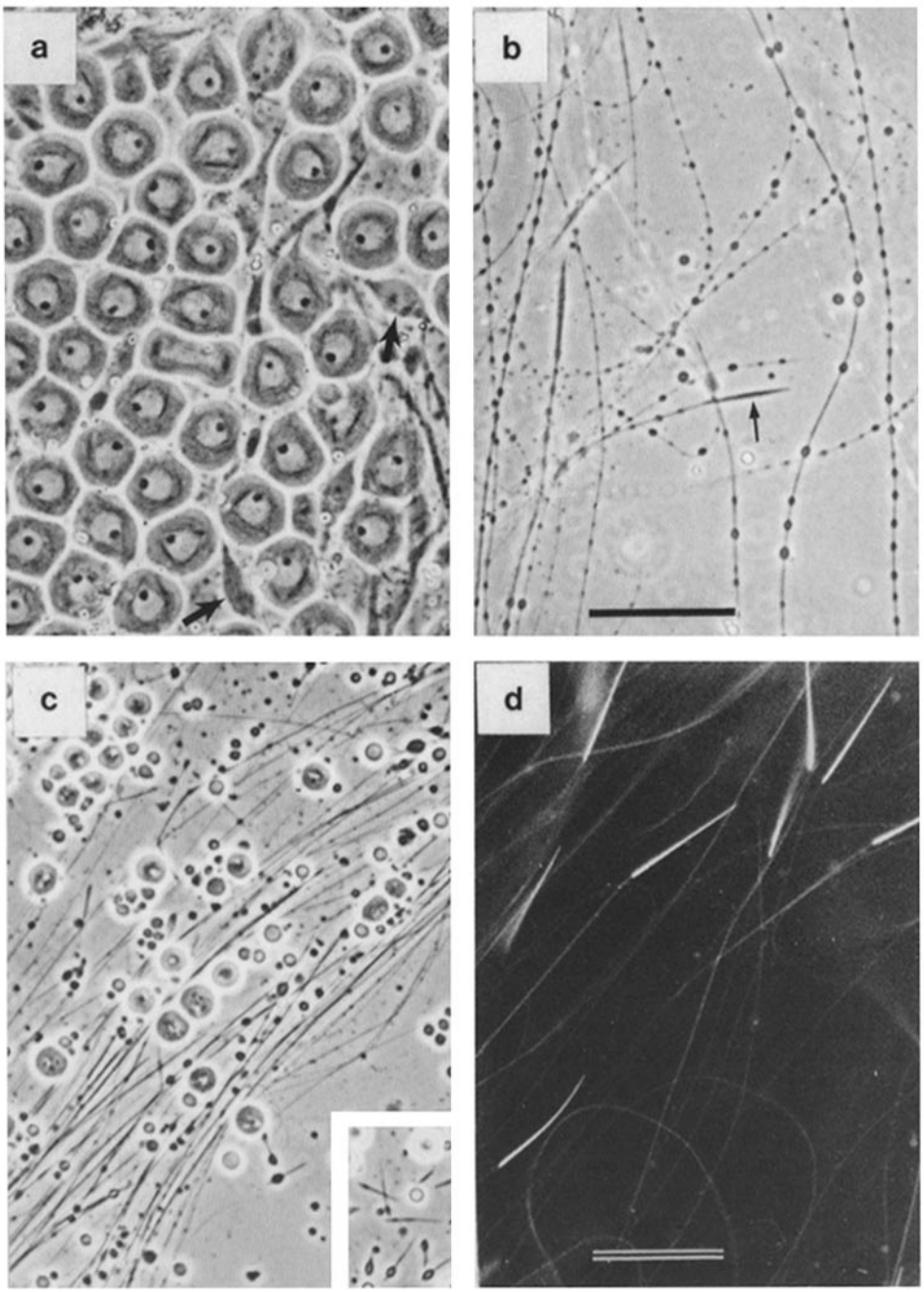

FIGURE 2 Micrographs of the four types of cell preparations that were used for SDS-PAGE analysis. (*a*) A phase-contrast micrograph illustrating a representative field of a typical spermatocyte preparation. Most of the cells are in prophase of meiosis I, but some are undergoing the first meiotic division, e.g., cytokinesis in the center and anaphase at the top. There are also a few young spermatids in this field (arrows). (*b*) Spermatids obtained from a pupa just after the pupal molt. At this stage, cell lengths range between 800 and 1,500 μm, the nuclei (arrow) are elongated, and surface blebs are apparent along the tails. (*c*) The contents of an adult testis containing sperm, refractile vesicles, and rod-shaped structures (shown in *inset*). (*d*) A fluorescence micrograph of sperm that were isolated from vas deferens, fixed in 4% glutaraldehyde in 0.1 cacodylate buffer, and stained for 10 min in 0.1% acridine orange. The needle-shaped nuclei appear extremely fluorescent. Mature sperm have no surface blebs and may be as long as 1,800 μm. All micrographs were made with a 16/0.40-neofluar objective. *a*, *b*, and *c* × 400. Bar in *b*, 50 μm. *d* × 600. Bar, 30 μm.

(Fig. 5*b*) represents ~0.7% of the total homogenate protein. The difference between unfractionated p43 and residual p43, 0.9%, is the fraction of the homogenate that was bound by DNase (Table II).

Buffer G-treated spermatid homogenates (Fig. 6*a*) were centrifuged for 3 h at 150,000 *g* to remove guanidine-insoluble particulate components that were present after the 2.5-h extraction period (Fig. 6*b*). Only high-speed supernatant fractions were applied to the column (Fig. 6*c*). All of the p43 in the supernate (0.8% of the total protein) was bound to the column (Figs. 6 and 7, Table II). DNase-bound spermatid protein was recovered as described above for spermatocytes. Gels of DNase-bound proteins from spermatids were identical to those from spermatocytes.

We also applied sperm homogenates prepared in buffer G to DNase affinity columns. Under the conditions of our assay, no

sperm polypeptides were observed to bind specifically to the DNase (data not shown).

To further characterize the p43 components isolated with DNase, we prepared two-dimensional peptide maps of radioiodinated DNase-isolated p43 bands and compared them with peptide maps of known actins and with maps of other proteins having molecular weights similar to actin. Although no pair of

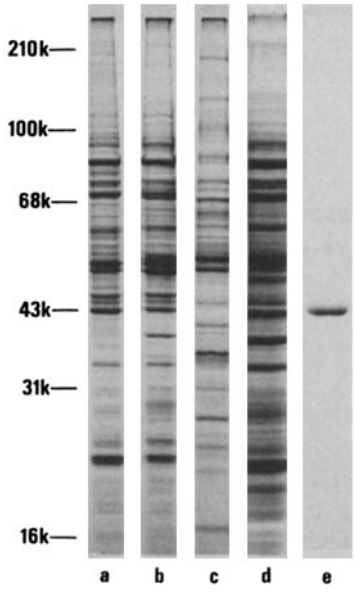

FIGURE 3 Results of SDS-PAGE analysis of preparations illustrated in Fig. 1. (*a*) Spermatocytes. (*b*) Spermatids. (*c*) Sperm. (*d*) Adult testes. (*e*) Rabbit muscle actin. About 10 μg of protein was loaded per lane. *a*, *b*, *c*, and *e* were taken from the same slab gel. Molecular weight standards were myosin (210,000), phosphorylase *a* (100,000), bovine serum albumin (68,000), rabbit muscle actin (43,000), DNase I (31,000), and myoglobin (16,000).

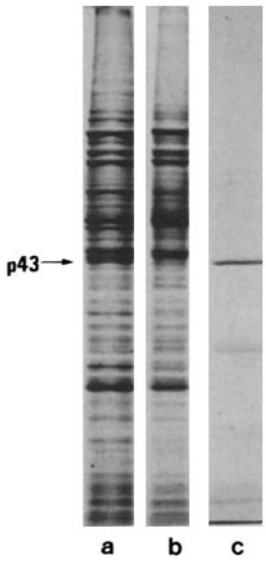

FIGURE 4 Gels of buffer G-treated spermatocyte homogenates: (*a*) before DNase chromatography, (*b*) after DNase chromatography (there is a residual p43 band), and (*c*) DNase-bound material that was removed from the column with 2% SDS.

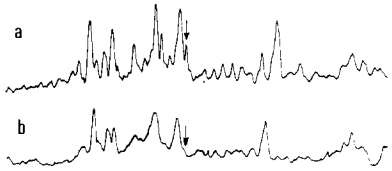

FIGURE 5 Densitometer scans of gels of buffer G-treated spermatocyte homogenates: (*a*) before DNase chromatography (there is a p43 band) and (*b*) after DNase chromatography (there is a reduction in the intensity of the p43 band). In this figure, and all subsequent gel scan figures, the arrows indicate the p43 band. Direction of electrophoresis is from left to right.

TABLE II

Summary of Results of Densitometer Scans of SDS Gels

Cell type/treatment	Total p43 (actin plus nonactin polypeptides)	Nonactin polypeptides	Actin (p43 minus nonactin polypeptides
Spermatocyte—buffer G			
Homogenate	1.6 ± 0.1 (14)	0.7 ± 0.1 (6)	0.9
Spermatocyte—buffer S			
Homogenate	1.4 ± 0.1 (14)		
Pellet	0.7 ± 0.1 (8)	None*	0.7
Supernate	0.7 ± 0.1 (8)	0.5 ± 0.1 (5)*	0.2
Spermatocyte—buffer S			
Unfractionated homogenate	1.5 ± 0.1 (3)	0.7 ± 0.1 (12)	0.8
Spermatid—buffer G			
Homogenate	1.5 ± 0.2 (13)		
Pellet	0.5 ± 0.1 (6)‡	Not determined	Not determined
Supernate	0.8 ± 0.1 (6)	None detected	0.8
Spermatid—buffer S			
Homogenate	1.6 ± 0.1 (8)		
Pellet	0.9 ± 0.1 (8)	Not determined	0.4‡
Supernate	0.7 ± 0.1 (8)	None detected	0.7

Data are expressed as the approximate percentage of total cell protein.

Cells were homogenized in either buffer G or buffer S, centrifuged for 3 h at 150,000 *g* when required, and the resulting solubilized preparations were run on DNase affinity columns. The amount of p43 was estimated densitometrically from gels of homogenates and fractionated homogenates run before (total p43) and after (nonactin polypeptides) DNase chromatography. The composition of each p43 was determined as outlined in Results.

* On the basis of results obtained from the spermatocyte—buffer S unfractionated homogenate experiment (Results), we conclude that the pellet consists of sedimentable actin and that residual polypeptides present in the supernate after DNase chromatography correspond to nonactin polypeptides identified in residual p43 of the buffer G experiments.

‡ Peptide analysis of the p43 polypeptide found in buffer G high-speed pellets reveals that 0.5% of the total homogenate protein contains nonactin and guanidine-insoluble actin. Because these components are also expected to pellet in the presence of buffer S, the increase in the amount of protein in buffer S pellet p43 band is concluded to be the result of sedimentable actin.

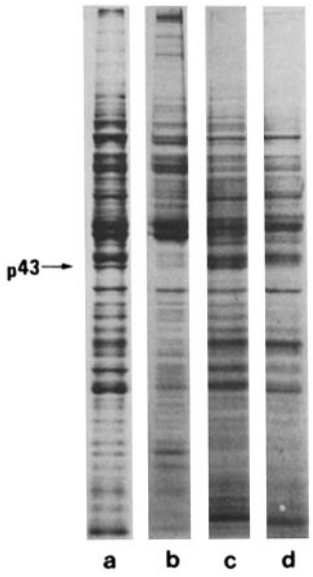

FIGURE 6 Gels of buffer G-treated spermatid homogenate and homogenate fractions: (*a*) homogenate, (*b*) high-speed pellet, (*c*) high-speed supernate before DNase chromatography, and (*d*) high-speed supernate after DNase chromatography showing the removal of p43.

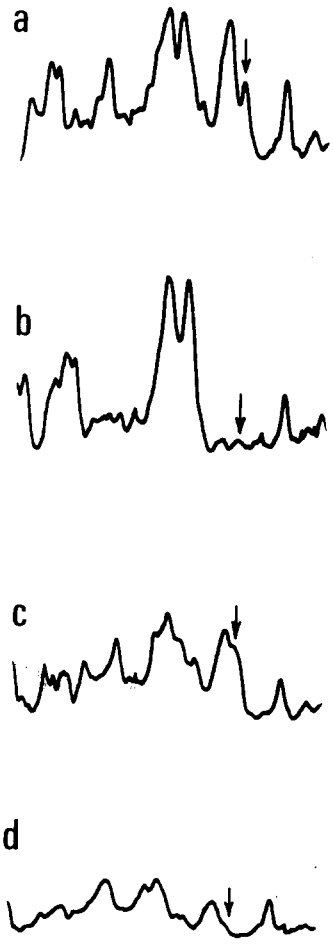

FIGURE 7 Densitometer scans of gels of buffer G-treated spermatid homogenate and homogenate fractions: (*a*) homogenate, (*b*) high-speed pellet, (*c*) high-speed supernate, and (*d*) high-speed supernate after DNase chromatography depicting the removal of p43. Only the 35,000–70,000-dalton region of the gel scan is illustrated.

these maps was identical, many similarities were observed among the peptide maps of the known actins (Fig. 8 *a–c*). No such homology was observed between any two maps of the other proteins investigated (Fig. 8 *e–g*) nor was there a significant likeness of any of these maps to a peptide map of a known actin. The peptide map of DNase-isolated spermatid p43 (Fig. 8 *d*) did, however, resemble the actin peptide maps. Because the tryptic peptide map of DNase-isolated spermatid p43 is virtually identical to the map of DNase-isolated spermatocyte p43 (Fig. 9 *b*) and because the peptide maps of both polypeptides seem to share some structural homologies with peptide maps of three previously characterized actins (36, 27, 30, 41, 37, 42), henceforth we will refer to these as spermatocyte and spermatid actin.

To determine the composition of the residual p43 band in unbound column fractions of spermatocyte homogenates, we prepared peptide maps of residual p43 for comparison with maps of spermatocyte actin and of unfractionated homogenate p43. The maps of spermatocyte actin (Fig. 9 *b*) and residual p43 (Fig. 9 *c*) were different and both appeared to be represented in the map of unfractionated p43 (Fig. 9 *a*). These results are important from three standpoints: (*a*) they suggest that residual p43 contains polypeptides other than actin (which we refer to as *nonactin*), (*b*) they show that all spermatocyte actin is converted to a form that binds DNase, and (*c*) they show

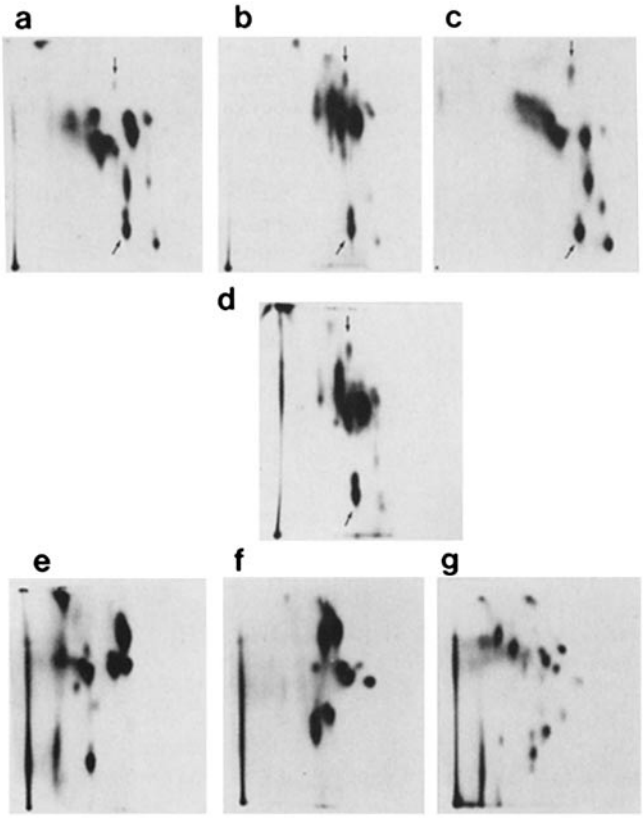

FIGURE 8 Autoradiograms of tryptic peptide maps of ^{125}I-labeled proteins: (*a*) rabbit skeletal muscle actin, (*b*) human erythrocyte actin, (*c*) actin extracted from *D. discoideum*, (*d*) DNase-isolated spermatid p43, (*e*) ovalbumin, (*f*) creatine kinse, and (*g*) α- and β-tubulin. The origin spots are at the lower left; peptides were electrophoresed in the horizontal and chromatographed in the vertical direction. Selected spots common to the actin maps are labeled with arrows. The acrylamide control for these maps is included in Fig. 9.

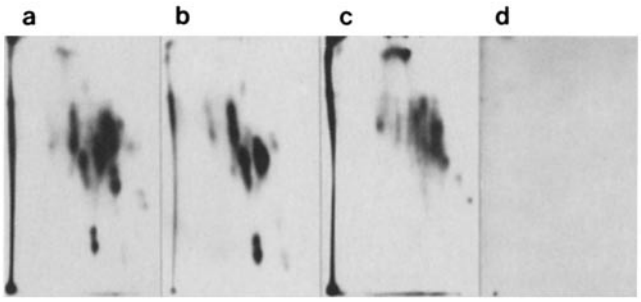

FIGURE 9 Autoradiograms of tryptic peptide maps of ^{125}I-labeled spermatocyte proteins; (*a*) homogenate p43, (*b*) DNase-isolated p43, (*c*) residual p43, and (*d*) a 10% polyacrylamide gel slice not containing a polypeptide. For *d*, a chromatogram was spotted with twice the largest volume used for extracts from a polypeptide-containing slice and electrophoresed, chromatographed, and autoradiographed as described (28). If a much larger sample volume is spotted or if autoradiographic exposures are longer (5–6 d instead of 12 h), distinct spots associated with acrylamide contaminants are visualized (see Fig. 2 of reference 28). However, this acrylamide map is very different from all the peptide maps presented here. Therefore, we conclude that the major spots and smears observed in the peptide maps are the result of polypeptides and are not caused by labeled acrylamide contaminants.

that treatment with mildly chaotropic buffer G does not adversely affect the binding properties of actin to DNase. A peptide map of the p43 band in high-speed pellets of buffer G-treated spermatids was similar to the map of the nonactin component of spermatocyte preparations (data not shown). However, unlike those of spermatocytes, maps of spermatid pellet p43 contained a trace amount of actin. This actin was not solubilized by treatment with 0.75 M guanidine and remained associated with other insoluble components during centrifugation. The basis for this apparent resistance to solubilization is not known. Because the amount of actin present in spermatid-buffer G pellets was difficult to assess by our methods, we have operationally defined the amount of assayable actin in spermatids to be 1%. This was determined by subtracting pellet p43 (0.5% of total protein and containing both nonactin polypeptides and guanidine-insoluble actin) from p43 of unfractionated homogenate (1.5% of total protein; Table II).

Having determined that ~1% of the total spermatocyte and spermatid protein is actin (Table II), we wanted to assess how much of the actin that we had isolated with buffer G actually existed in the monomeric form in vivo. To do that, we prepared homogenates in buffer S, which has been shown by Blikstad et al. (3) to provide ionic conditions which stabilize supramolecular forms of actin in their native state. Two control experiments were performed to test the possible effects of buffer S on actin polymerization and stability under the conditions that were used for our analysis. First, we wanted to know whether actin monomers might be induced to polymerize in buffer S during the 2.5-h extraction period at 4°C used to solubilize the cells. Viscometric analysis of rabbit muscle actin (Fig. 10) indicated that the polymerization of G-actin did not occur at concentrations <0.8 mg/ml, which is at least two orders of magnitude greater than the actin concentration in our cell homogenates (5 μg/ml for spermatocytes and 8 μg/ml for spermatids). It is important to emphasize that our data were obtained after only a 2.5-h incubation and thus are not comparable to values for the equilibrium critical monomer concentration reported by other investigators (14). Another consideration is that we used muscle actin in our control experiments. Because the polymerization properties of purified muscle and nonmuscle actin have been shown to be qualitatively similar (14), it seems unlikely that artefactual polymerization of gonial cell G-actin could have occurred under the conditions that we used in our analysis.

Since there have been reports that F-actin may depolymerize at low temperatures under certain ionic conditions (1, 13), we also investigated the effects of low temperature on preformed F-actin in buffer S (Fig. 11). We did not detect any decrease in the viscosity of rabbit muscle F-actin during a 2.5-h incubation at 4°C. Blikstad et al. (3) reported a similar stability for polymerized nonmuscle actin in buffer S. Taken together, the results suggest that low temperature effects under the conditions of our assay are negligible. Another detail that we considered was the possible influence of Triton X-100 on F-actin, but the results of other researchers (40, 5) indicate that this is unlikely.

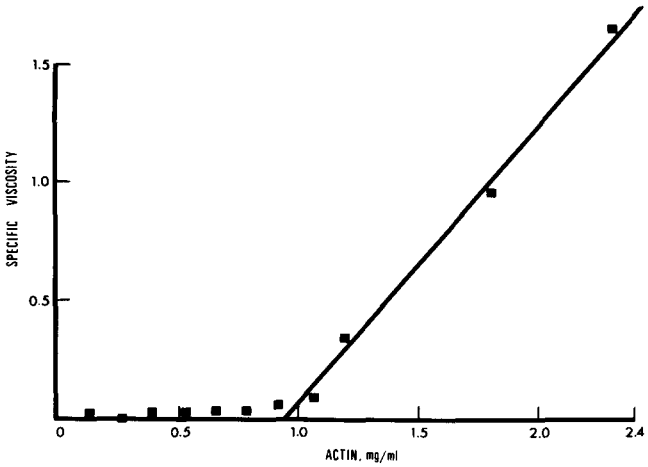

FIGURE 10 The polymerization of G-actin in buffer S during a 2.5-h incubation at 0–4°C. Lyophilized G-actin, prepared from rabbit skeletal muscle acetone powder (36), was first dialyzed for 24 h at 0–4°C against 500 vol of 5 mM Tris-HCl, 0.2 mM ATP, 0.2 mM DDT, pH 7.6. After a 3-h centrifugation at 100,000 *g*, the clarified G-actin supernate was diluted to the indicated protein concentration with the buffer just described and made 0.15 M in NaCl and 2 mM in $MgCl_2$. After a 2.5-h incubation at 0–4°C, the viscosity of the actin was measured in a size 150 Cannon-Manning semi-microviscometer (Cannon Instrument Co., State College, Pa.).

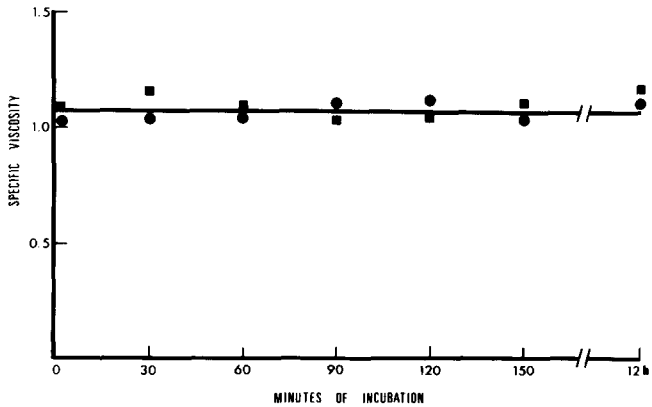

FIGURE 11 The effect of low temperature on F-actin prepared in buffer S. A 1.4-mg/ml solution of G-actin, prepared as described in Fig. 10, was polymerized to F-actin in buffer S for 7 h at 27°C, after which the viscosity of the F-actin was measured at various times during a 2.5-h incubation at either 25°C (■) or 4°C (●).

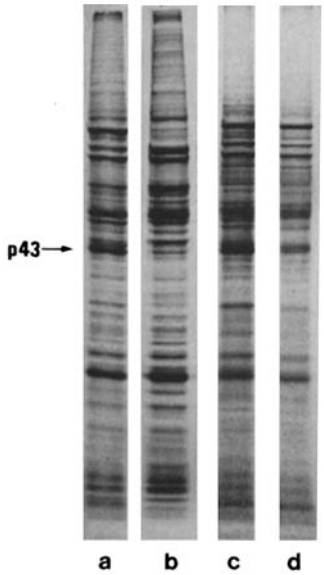

FIGURE 12 Gels of buffer S-treated spermatocyte homogenate and homogenate fractions: (*a*) homogenate, (*b*) high-speed pellet, (*c*) high-speed supernate, and (*d*) high-speed supernate after passage through DNase (there is a residual p43 band).

Our assay for native monomeric actin included a high-speed centrifugation step to clarify homogenates of supramolecular forms of actin that might bind to the DNase (18, 3) or collect nonspecifically in the agarose bead matrix of our columns. Details regarding the efficiency of the centrifugation step are presented in Methods. Three fractions were collected for analysis: (*a*) the high-speed pellet, which contained sedimentable actin and was not applied to DNase columns, (*b*) the high-speed supernate, which was applied to DNase columns, and (*c*) the unbound column fraction, which represented the high-speed supernate after passage through the affinity column. Nonsedimentable actin that was bound to the column under the conditions of our assay was assumed to be in the monomeric state.

The polypeptide composition of the three fractions described above is illustrated in Fig. 12 (spermatocytes) and 14 (spermatids). Analysis of gel scans of both spermatocyte and spermatid pellet fractions (Figs. 12*b* and 13*b*, 14*b* and 15*b*) indicated that ~0.7% of the spermatocyte homogenate and 0.9% of spermatid homogenate was sedimentable p43 (Table II). The high-speed supernatant fraction (Figs. 12*c* and 13*c*, 14*c* and 15*c*) of both cell types contained p43 polypeptides before DNase chromatography (0.7% in both cell types), but only the unbound spermatocyte column fraction contained p43 after DNase chromatography (cf. Figs. 12*c* and *d* with 14*c* and *d*; 13*c* and *d* with 15*c* and *d*; refer to Table II). Although this suggested that all of the p43 of spermatid high-speed supernate was monomeric actin, the p43 band remaining after DNase chromatography of high-speed supernates of spermatocytes indicated that only a fraction of the p43 in the supernate, amounting to ~0.2% of the total homogenate protein, was monomeric actin. Gel scans revealed that the amount of unbound p43 present in spermatocyte column fractions was 0.5 ± 0.1%, which was comparable to the amount of residual p43 (0.7 ± 0.1%) estimated in buffer G experiments. Whereas these results tended to support the possibility that the unbound p43 in column fractions of spermatocyte high-speed supernates could represent nonactin polypeptides identified in peptide maps of buffer G residual p43 (Fig. 9*c*), it was also possible

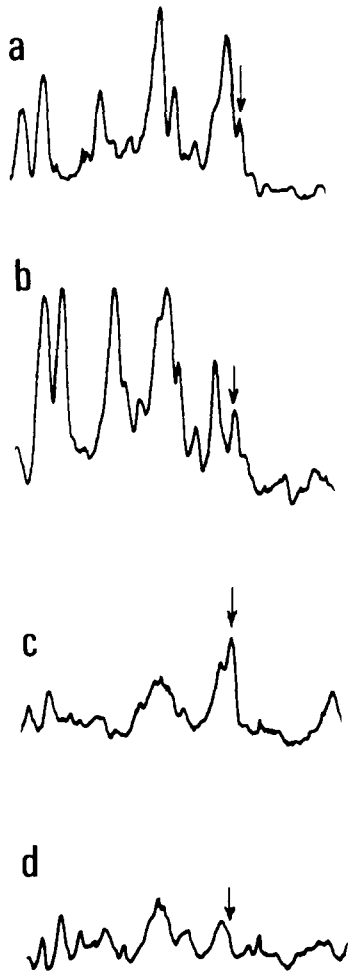

FIGURE 13 Densitometer scans of gels of buffer S-treated spermatocyte homogenate and homogenate fractions: (*a*) homogenate, (*b*) high-speed pellet, (*c*) high-speed supernate showing a prominent p43 band, and (*d*) high-speed supernate after passage through DNase (a residual p43 band is observed). Only the 35,000–70,000-dalton region of the gel scan is illustrated.

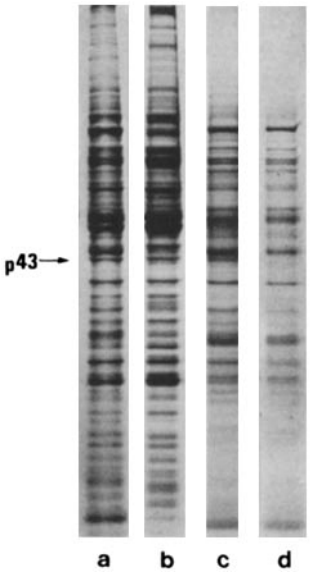

FIGURE 14 Gels of buffer S-treated spermatid homogenate and homogenate fractions: (*a*) homogenate, (*b*) high-speed pellet, (*c*) high-speed supernate, and (*d*) high-speed supernate after passage through DNase (there is no p43 band).

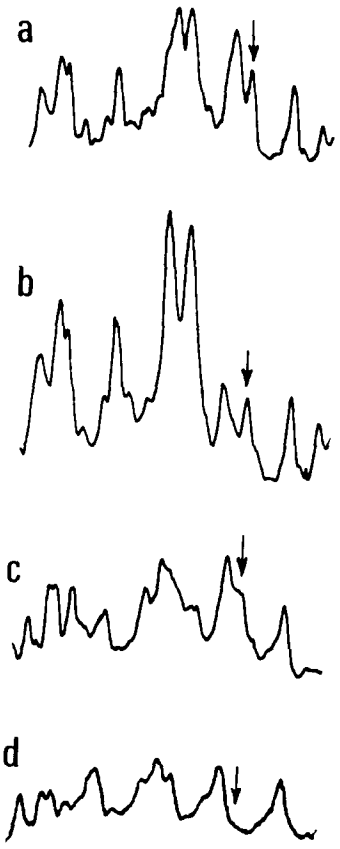

FIGURE 15 Densitometer scans of gels of buffer S-treated spermatid homogenate and homogenate fractions: (*a*) homogenate, (*b*) high-speed pellet (comparison of this scan with scans obtained from buffer G experiments [Fig. 7 *b*] reveals that considerably more protein is obtained in the buffer S pellet fraction when compared with pellets obtained from homogenates prepared in the more chaotropic buffer G. For example, compare the peaks to the left of p43 in Figs. 15 *b* and 7 *b*), (*c*) high-speed supernate, and (*d*) high-speed supernate after passage through DNase (all p43 is removed by this treatment). Only the 35,000-70,000-dalton region of the gel scan is illustrated.

that unbound p43 represented a nonsedimentable form of actin that did not bind DNase under the conditions of our assay. Because buffer S provides ionic conditions that stabilize supramolecular forms of actin, we would expect that interactions between actin and accessory proteins should be preserved. Likewise, it also seems reasonable that nonsedimentable actin could be complexed with accessory proteins that could sterically inhibit the interaction between actin and DNase (32). It seems unlikely that the actin in the unbound fraction could be denatured actin, because actin treated with 0.75 M guanidine retains its DNase-binding activity. The actual identification of unbound column fraction p43 and spermatocyte pellet p43 required further investigation.

To approach the question of whether there may be an inhibitory factor in buffer S-treated spermatocyte homogenates that could affect the DNase-binding activity of actin under the conditions of our assay, we analyzed unfractionated buffer S-treated spermatocyte homogenates using DNase affinity techniques. In this experiment, homogenates first were loaded onto the DNase column and eluted with buffer S. Then, to insure against nonspecific binding of p43 to the column, one bed volume of buffer G was applied to the column and the column flow was stopped for 2.5 h before elution with additional buffer G. The density of p43 in the unbound fraction eluted with buffer S was reduced significantly (Fig. 16 *a* and *b*). As was observed in buffer G experiments after DNase chromatography, 0.7 ± 0.1% of the total protein was found in p43 of the unbound fraction. Analysis of fractions eluted with buffer G revealed no additional p43 polypeptides (Fig. 16 *c*). Passage of 2% SDS through the column resulted in the removal of DNase-bound actin (Fig. 16 *d*). We conclude from these results that the composition of unbound p43 in experiments with buffer S-treated spermatocytes (Figs. 12 and 16) represents nonactin polypeptides identified in buffer G experiments and that p43 in high-speed pellets of buffer S-treated spermatocytes is sedimentable actin. In addition, it is apparent that accessory polypeptides that may be associated with sedimentable and/or nonsedimentable actin in buffer S-treated spermatocyte homogenates do not preclude the binding of actin to DNase under conditions of our assay.

In conclusion, a comparison of the results from buffer G and buffer S experiments suggests that the amount of monomeric actin in spermatocytes is different from that in spermatids (Table II). About 0.2% of the total spermatocyte homogenate was bound to DNase after the homogenate had been fractionated by centrifugation and the supernate passed through a DNase column. Under identical experimental conditions, spermatid p43 was found to contain a greater proportion of monomeric actin; 0.7% of the homogenate was capable of binding DNase. Because our analysis of gel scans indicates that actin comprises ~1% of the total cell protein in both cell types, the above differences suggest that only ~20% of the actin of spermatocytes is monomeric and that ~70% of the assayable spermatid actin is monomeric.

DISCUSSION

We have described in this report an approach that combines DNase affinity chromatography and two-dimensional peptide

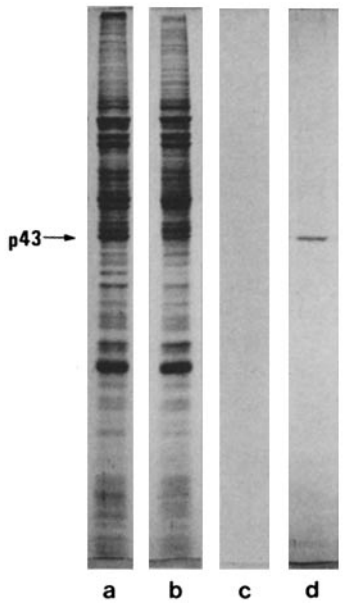

FIGURE 16 Gels of buffer S-treated spermatocytes that were not fractionated by centrifugation before DNase chromatography: (*a*) homogenate, (*b*) homogenate after DNase chromatography (there is a reduction in the amount of p43), (*c*) buffer G fraction (elution after incubation for 2.5 h at 4°C removes no additional p43 polypeptides), and (*d*) DNase-bound polypeptide that was removed from the column with 2% SDS.

mapping to assess the actin content of crane-fly gonial cells. This method has enabled us to identify the polypeptide components of gel slices that contain as little as 0.1 μg of protein. This procedure may be applicable to other systems in which only submicrogram amounts of protein are available for analysis.

Our data not only confirm some of the previous ultrastructural findings presented by Forer and Behnke (11, 12) but they also provide new information on the amounts and organization of actin in these cells. In contrast to Forer and Behnke's report (12), we did not detect any protein co-migrating with rabbit muscle actin in our SDS gels of mature sperm. The apparent discrepancy between the results of our analysis of sperm and those of Forer and Behnke can be explained simply in terms of the materials used. Our preparations of sperm were obtained from vas deferens whereas Forer and Behnke used adult testes as their source of sperm. Because adult testes contain numerous vesicular and rod-shaped components, in addition to sperm, and because SDS gels of adult testes reveal a prominent p43 band, we suggest that the actin detected by Forer and Behnke probably was derived from other components.

Although we have not characterized all of the components in adult testes, the morphological similarity between the vesicular components found in the adult testis (Fig. 2*c*) and the vesicular blebs observed along the tails of spermatids (Fig. 2*b*) suggests that testicular vesicles actually may be spermatid components that were eliminated during spermiogenesis (4). Accordingly, on the basis of the absence of both vesicular blebs and actin in sperm and the presence of a large p43 band in SDS gels of whole adult testes preparations, we believe it is reasonable to suggest that the vesicular components of adult testes contain actin.

Actin comprises ~1% of the protein of both spermatocyte and spermatid homogenates and is present in both cells in sedimentable and nonsedimentable forms. Because nonsedimentable actin which binds DNase under the conditions of our assay is assumed to be monomeric, the results of our actin assay indicate that there is proportionately more monomeric actin in spermatids than in spermatocytes. The presence of significant amounts of sedimentable actin in spermatocyte homogenates suggests that it is in either a polymerized or an aggregated state. Although the significance of these differences between the two cell types is not clear, they may be related to the physiological requirements of these cells during spermiogenesis. For example, spermatocytes undergo two rounds of cytokinesis before becoming spermatids. In view of the well-documented role of actin in cytokinesis (33), it seems reasonable that spermatocyte actin may be organized into supramolecular structures that facilitate the cleavage process. The maturation of spermatocytes into spermatids is accompanied by an increase in the amount of monomeric actin. This change may be related to dynamic molecular events associated with the morphological changes observed at this stage of spermiogenesis. A characteristic feature of spermatids is the existence of numerous blebs along their tails. Actin could play an active role in the formation and/or transport of these blebs. It is also possible that unpolymerized actin could be sequestered within the blebs and eliminated along with other extraneous cytoplasmic components as an inactive by-product of spermiogenesis (4). Clearly, more information regarding the intracellular localization and precise organization of actin in these cells is needed before conclusions regarding the significance of these differences can be drawn.

Our finding that only ~1% of the total spermatocyte and spermatid protein is actin imposes certain limitations on its intracellular distribution. If we assume that (*a*) actin is distributed evenly among all the cells of a homogenate and that (*b*) the sedimentable actin we detected with the selective actin assay is F-actin, then it should be possible to make a theoretical estimation of the F-actin content per cell. Confining this discussion to primary spermatocytes, there would be 6.7×10^{-17} mol of sedimentable actin per cell. This would correspond to 1.1×10^{5} μm of F-actin, or 4,400 filaments each having the length of the cell (25 μm). Indeed, actin filaments have been observed in spermatocytes after treatment with glycerol and heavy meromyosin (11). However, based on the values presented above, the apparent absence of dense arrays of actin filaments in either conventionally prepared spermatocytes (11) or in spermatocytes fixed without osmium (25, 26) suggests that if actin filaments are present in these cells, they must be sparsely distributed and not readily visualized unless background cytoplasm is extracted with glycerol. Alternatively, it is possible that sedimentable actin may be organized in a more labile, amorphous state, such as a gelled meshwork, which could be transformed into free, recognizable filaments by treatment with either glycerol or heavy meromyosin. In view of the potentially complicating influences that glycerol (22) and heavy meromyosin (45, 38) could have on G-actin or labile states of actin (41), we currently are attempting to approach questions concerning the intracellular distribution of actin in spermatocytes and spermatids using alternative, less perturbing techniques.

Finally, results from our two-dimensional peptide analysis have shown that although homologies are apparent between maps of different actins, each pattern displays unique aspects as well. In view of these differences, the similarity between the maps of actin from spermatocytes and spermatids and the map of human erythrocyte actin is most striking. As a step toward understanding the relationship between peptide maps and protein function, we plan to extend our peptide analysis to include actins from other sources. The similarity of maps of gonial cell actin to erythrocyte actin, which is a major component of the erythrocyte cortex (41, 15), has led us to explore the possible association between actin and the cell cortex of spermatocytes and spermatids. Using a combined structural and biochemical approach, including scanning electron microscopy and the use of photoactivated cross-linking reagents, we are hopeful that results obtained with these techniques will be useful in resolving both the distribution and the precise state of organization of actin in these cells.

This work was done during a sabbatical year spent by J. R. LaFountain and A. R. Strauch at Harvard University in the laboratory of D. Lansing Taylor, and the authors thank him for providing the facilities and support needed to bring this investigation to completion. We also want to thank Margaret Taylor for her help in making the stay in the Boston area a very pleasant one. The assistance and generosity of the Taylor group, and in particular of Velia Fowler and Skip Virgin for providing gel slices of erythrocyte and *Dictyostelium* actin, is gratefully acknowledged, and we thank Professors Daniel Branton, Carroll M. Williams, and Lawrence Bogorad for the use of facilities in their laboratories.

This work was supported by grants from the National Science Foundation to J. R. LaFountain (PMC 75-13954) and to D. L. Taylor (PCM 78-22499) and from the National Institute of Health to D. L. Taylor (AM 18111). E. J. Luna was an NIH Postdoctoral Fellow (HL 05555) at the time of this investigation.

Received for publication 17 January 1980, and in revised form 24 March 1980.

REFERENCES

1. Asakura, S., M. Kasai, and F. Oosawa. 1960. The effect of temperature on the equilibrium state of actin solutions. *J. Polym. Sci. Part D Macromol. Rev.* 44:35–49.
2. Bennett, V., and D. Branton. 1977. Selective association of spectrin with the cytoplasmic surface of human erythrocyte plasma membranes. *J. Biol. Chem.* 252:2753–2763.
3. Blikstad, I., F. Markey, L. Carlsson, T. Persson, and U. Lindberg. 1978. Selective assay of monomeric and filamentous actin in cell extracts using inhibition of deoxyribonuclease I. *Cell.* 15:935–943.
4. Bowen, R. H. 1920. Studies on insect spermiogenesis I. The history of the cytoplasmic component of the sperm in hemiptera. *Biol. Bull. (Woods Hole).* 39:316–363.
5. Bray, D., and C. Thomas. 1976. Unpolymerized actin in fibroblasts and brain. *J. Mol. Biol.* 105:527–544.
6. Buckley, I. K., and K. Porter. 1967. Cytoplasmic fibrils in living cultured cells. A light and electron microscope study. *Protoplasma.* 64:349–380.
7. CIBA Foundation Symposium. 1973. Locomotion of Tissue Cells, Number 14. American Elsevier Publishing Co., Inc., New York.
8. Elder, J. H., R. A. Pickett, II, J. Hampton, and R. A. Lerner. 1977. Radioiodination of proteins in single polyacrylamide gel slices-tryptic peptide analysis of all the major members of complex multicomponent systems using microgram quantities of total protein. *J. Biol. Chem.* 252:6510–6515.
9. Forer, A. 1964. Evidence for two spindle fiber components: a study of chromosome movement in living crane-fly (*Nephrotoma suturalis*) spermatocytes using polarization microscopy and an ultraviolet microbeam. Ph.D. thesis. Dartmouth College, Hanover, N. H.
10. Forer, A. 1974. Possible roles of microtubules and actin-like filaments during cell division. *In* Cell Cycle Controls. G. M. Padilla, I. L. Cameron, and A. M. Zimmerman, editors. Academic Press, Inc., New York.
11. Forer, A., and O. Behnke. 1972. An actin-like component in spermatocytes of a crane fly (*Nephrotoma suturalis* Loew). II. The cell cortex. *Chromosoma (Berl.).* 39:175–190.
12. Forer, A., and O. Behnke. 1972. An actin-like component in sperm tails of a crane fly (*Nephrotoma suturalis* Loew). *J. Cell Sci.* 11:491–519.
13. Gordon, D. J., Y. Z. Wang, and E. D. Korn. 1976. Polymerization of *Acanthamoeba* actin. Kinetics, thermodynamics and co-polymerization with muscle actin. *J. Biol. Chem.* 251: 7474–7479.
14. Gordon, D. J., J. L. Boyer, and E. D. Korn. 1977. Comparative biochemistry of non-muscle actins. *J. Biol. Chem.* 252:8300–8309.
15. Hainfeld, J. F., and T. L. Steck. 1977. The submembrane reticulum of the human erythrocyte: a scanning electron microscope study. *J. Supramol. Struct.* 6:301–311.
16. Halsall, H. B. 1967. Atassi-Gandhi sedimentation coefficient and molecular weight relationships. *Nature (Lond.).* 215:880–881.
17. Hellewell, S. B., and D. L. Taylor. 1979. The contractile basis of amoeboid movement VI. The solation-contraction coupling hypothesis. *J. Cell Biol.* 83:633–648.
18. Hitchcock, S. E., L. Carlsson, and U. Lindberg. 1976. Depolymerization of F-actin by deoxyribonuclease I. *Cell.* 7:531–542.
19. Huxley, H. E. 1963. Electron microscope studies on the structure of natural and synthetic filaments from striated muscle. *J. Mol. Biol.* 7:281–308.
20. Ishikawa, H., R. Bischoff, and H. Holtzer. 1969. Formation of arrowhead complexes with heavy meromyosin in a variety of cell types. *J. Cell Biol.* 43:312–328.
21. Kahn, R., and R. W. Rubin. 1975. Quantitation of submicrogram amounts of protein using Coomassie brilliant blue R on sodium dodecyl sulfate-polyacrylamide slab gels. *Anal. Biochem.* 67:347–352.
22. Kasai, M., E. Nakand, and F. Oosawa. 1965. Polymerization of actin free from nucleotides and divalent cations. *Biochim. Biophys. Acta.* 94:494–503.
23. Kidd, G. H., R. E. Hunt, M. L. Boeshore, and L. H. Pratt. 1978. Asymmetry of the primary structure of undegraded phytochrome. *Nature (Lond.).* 276:733–735.
24. Laemmli, U. K. 1970. Cleavage of structural proteins during the assembly of the head of bacteriophage T4. *Nature (Lond.).* 227:680–685.
25. LaFountain, J. R., Jr. 1975. What moves chromosomes, microtubules or microfilaments? *Biosystems.* 7:363–369.
26. LaFountain, J. R., Jr., C. R. Zobel, H. R. Thomas, and C. Galbreath. 1977. Fixation and staining of F-actin and microfilaments using tannic acid. *J. Ultrastruct. Res.* 58:78–86.
27. Lazarides, E., and U. Lindberg. 1974. Actin is the naturally occurring inhibitor of deoxyribonuclease I. *Proc. Natl. Acad. Sci. U.S.A.* 71:4742–4746.
28. Luna, E. J., G. H. Kidd, and D. Branton. 1979. Identification by peptide analysis of the spectrin-binding protein in human erythrocytes. *J. Biol. Chem.* 254:2526–2532.
29. March, S. C., I. Parikh, and P. Cuatrecasas. 1974. A simplified method for cyanogen bromide activation of agarose for affinity chromatography. *Anal. Biochem.* 60:149–152.
30. Nakashima, K., and E. Beutler. 1979. Comparison of structure and function of human erythrocyte and human muscle actin. *Proc. Natl. Acad. Sci. U.S.A.* 76:935–938.
31. Pollard, T. D., and R. R. Weihing. 1974. Actin and myosin in cell movements. *Crit. Rev. Biochem.* 2:1–65.
32. Rohr, G., and H. G. Mannherz. 1979. The activation of actin: DNase I complex with rat liver plasma membranes. The possible role of 5′-nucleotidase. *FEBS (Fed. Eur. Biochem. Soc.) Lett.* 99:351–356.
33. Schroeder, T. E. 1975. Dynamics of contractile ring. *In* Molecules and Cell Movement. S. Inoue and R. E. Stephens, editors. Raven Press, New York. 305–334.
34. Sloboda, R. D., W. L. Dentler, and J. L. Rosenbaum. 1976. Microtubule-associated proteins and the stimulation of tubulin assembly *in vitro*. *Biochemistry.* 15:4497–4505.
35. Spooner, B. 1975. Microfilaments, microtubules and extracellular materials in morphogenesis. *Bioscience.* 25:440–451.
36. Spudich, J. A., and S. Watt. 1971. The regulation of rabbit skeletal muscle contraction. *J. Biol. Chem.* 246:4866–4871.
37. Spudich, J. A. 1974. Biochemical and structural studies of actomyosin-like proteins from non-muscle cells. *J. Biol. Chem.* 249:6013–6020.
38. Tawada, K., and F. Oosawa. 1969. Effect of the H-meromyosin plus ATP system on F-actin. *Biochim. Biophys. Acta.* 180:199–201.
39. Taylor, D. L., and J. S. Condeelis. 1979. Cytoplasmic structure and contractility in amoeboid cells. *Int. Rev. Cytol.* 56:57–144.
40. Tilney, L. G., S. Hatano, K. Ishikawa, and M. Mooseker. 1973. The polymerization of actin: its role in the generation of the acrosomal process of certain echinoderm sperm. *J. Cell Biol.* 59:109–126.
41. Tilney, L. G., and P. Detmers. 1975. Actin in erythrocyte ghosts and its association with spectrin. Evidence for a nonfilamentous form of these two molecules *in situ*. *J. Cell Biol.* 66:508–520.
42. Uyemura, D. G., S. S. Brown, and J. A. Spudich. 1978. Biochemical and structural characterization of actin from *Dictyostelium discoideum*. *J. Biol. Chem.* 253:9088–9096.
43. Weisenberg, R. C. 1972. Microtubule-formation *in vitro* in solutions containing low calcium concentration. *Science (Wash. D.C.).* 177:1104–1105.
44. Wigglesworth, V. B. 1966. Insect Physiology. 6th edition, Methuen, London.
45. Yagi, K., R. Mase, I Sakakibara, and H. Asai. 1965. Function of heavy meromyosin in the acceleration of actin polymerization. *J. Biol. Chem.* 240:2448–2454.